ARTICLE

Quasi-Classical Trajectory Study on O^++DH (v=0, j=0)→OD^++H Reaction at Different Collision Energy

Hai-zhu Sun, Xin-guo Liu*, Juan-juan Lv, Hui-rong Liu

College of Physics and Electronics, Shandong Normal University, Ji'nan 250014, China

(Dated: Received on May 18, 2010; Accepted on June 23, 2010)

The quasi-classical trajectory calculations O^++DH(v=0, j=0)→OD^++H reactions on the RODRIGO potential energy surface have been carried out to study the isotope effect on stereo-dynamics at the collision energies of 1.0, 1.5, 2.0, and 2.5 eV. The distributions of dihedral angle $P(\phi_r)$ and the distributions of $P(\theta_r)$ are discussed. Furthermore, the angular distributions of the product rotational vectors in the form of polar plot in θ_r and ϕ_r are calculated. The differential cross section shows interesting phenomenon that the reaction is dominated by the direct reaction mechanism. Reaction probability and reaction cross section are also calculated. The calculations indicate that the stereo-dynamics properties of the title reactions are sensitive to the collision energy.

Key words: Stereo-dynamics, Quasi-classical trajectory method, Polarization-dependent differential cross-section

I. INTRODUCTION

Ion-molecule reactions are relevant in a number of interesting situations including interstellar chemistry, electric discharges, and planetary ionospheres. The reactive system O^++DH(v=0, j=0)→OD^++H, which is selected, is an exceptional case of ion-molecule reaction and is important in interstellar chemistry and in the Earth's ionosphere. Thus, it can be regarded as a prototype of moderately exothermic ion-molecule reactions involving a H atom transfer and it takes place adiabatically on the ground PES ($1^4A''$ surface in C_s symmetry) in a wide collision energy (E_T, relative translational energy) interval [1−4]. Reaction O^++HH(v=0, j=0)→OH^++H is important in dense interstellar clouds, where subsequent reactions of OH^+ with H_2 lead to the formation of H_2O^+ and H_3O^+ molecular ions [5].

In 2004, Rodrigo *et al.* published the most accurate PES for O^++HH→OH^++H reaction [6]. After that, there are many theoretical and experimental works for O^++HH→OH^++H reaction and its isotopic variants [5,8,9]. Rodrigo *et al.* studied the cross section, maximum impact parameter and reaction probability of the O^++HH→OH^++H reaction using the quasi-classical trajectory method [5], and the results were in excellent accordance with the experimental results, which were taken from Burley *et al.* [7]. Also, Rodrigo *et al.* studied the integral cross sections of the O^++HH(v=0, j=0)→OH^++H reaction using the close-coupling hyper-spherical (CCH) exact quantum method and compared with the quasi-classical trajectory method [8]. Rodrigo *et al.* again using the time dependent real wave packet method studied the reaction O^++HH(v=0, j=0)→OH^++H, and its isotopic variants [9].

There are many studies about the reaction O^++HH and its isotopic variants (D_2, HD), but little for the isotopic variants DH. In order to obtain more information of this system, we investigated the reaction O^++DH(v=0, j=0)→OD^++H by the quasi-classical trajectory (QCT) method.

II. THEORY

A. Vector correlation among k, k′, and j′

The center-of-mass frame (shown in Fig.1) is chosen in this work. The reagent relative velocity vector **k** is parallel to the z-axis, and x-z plane is the scattering

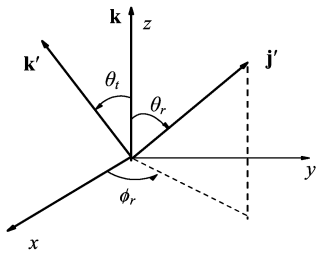

FIG. 1 The center-of-mass coordinate system used to describe the **k**, **k**′, and **j**′ correlations.

*Author to whom correspondence should be addressed. E-mail: liuxinguo@sdnu.edu.cn, Tel.: +86-531-86180892

plane containing the initial and final relative velocity vectors $\mathbf{k}$ and $\mathbf{k}'$. θ_t is called scattering angle, which is the angle between $\mathbf{k}$ and $\mathbf{k}'$. θ_r and ϕ_r are the polar and azimuthal angles of the final rotational momentum $\mathbf{j}'$.

Usually, two vector correlations ($\mathbf{k}$-$\mathbf{j}'$, $\mathbf{k}$-$\mathbf{k}'$, or $\mathbf{k}'$-$\mathbf{j}'$) can be expanded into a series of Legendre polynomials. The polar angle distribution function $P(\theta_r)$ describing the $\mathbf{k}$-$\mathbf{j}'$ correlation can be expanded in a series of Legendre polynomials as [10−24]

$$P(\theta_r) = \frac{1}{2}\sum_k (2k+1)a_0^{(k)} P_k(\cos\theta_r) \tag{1}$$

$$\begin{aligned} a_0^{(k)} &= \int_0^{\pi} P(\theta_r) P_k(\cos\theta_r)\sin\theta_r \mathrm{d}\theta_r \\ &= \langle P_k(\cos\theta_r)\rangle \end{aligned} \tag{2}$$

The expanding coefficients $a_0^{(k)}$ are called orientation (k is odd) and alignment (k is even) parameter.

The dihedral angle distribution function $P(\phi_r)$ describing $\mathbf{k}$-$\mathbf{k}'$-$\mathbf{j}$ correlation can be expanded in Fourier series as

$$\begin{aligned} P(\phi_r) = \frac{1}{2\pi}\Bigg(1 + \sum_{\text{even, } n\geq 2} a_n \cos n\phi_r + \\ \sum_{\text{odd, } n\geq 1} b_n \sin n\phi_r\Bigg) \end{aligned} \tag{3}$$

$$a_n = 2\langle \cos n\phi_r\rangle \tag{4}$$

$$b_n = 2\langle \sin n\phi_r\rangle \tag{5}$$

In this calculation, $P(\phi_r)$ is expanded up to n=24, which shows good convergence. The joint probability density function of angles θ_r and ϕ_r, which defines the direction of $\mathbf{j}'$, can be written as

$$\begin{aligned} P(\theta_r,\phi_r) &= \frac{1}{4\pi}\sum_{kq}[k]a_q^k C_{kq}(\theta_r,\phi_r)^* \\ &= \frac{1}{4\pi}\sum_k\sum_{q\geq 0}\Big[(a_{q\pm}^k \cos q\phi_r - \\ &\quad a_{q\mp}^k i\sin q\phi_r)C_{kq}(\theta_r,0)\Big] \end{aligned} \tag{6}$$

where C_{kq} are modified spherical harmonics. The polarization parameter is evaluated as

$$a_{q\pm}^k = 2\langle C_{k|q|}(\theta_r,0)\cos q\phi_r\rangle, \quad (k \text{ is even}) \tag{7}$$

$$a_{q\mp}^k = 2i\langle C_{k|q|}(\theta_r,0)\sin q\phi_r\rangle, \quad (k \text{ is odd}) \tag{8}$$

In the calculation, $P(\theta_r,\phi_r)$ is expanded up to k=7, which is sufficient for good convergence.

B. Polarization dependent differential cross sections

The fully correlated center-of-mass (CM) angular distribution is written as the sum [26]

$$P(\omega_t,\omega_r) = \sum_{kq}\frac{[k]}{4\pi}\frac{1}{\sigma}\frac{\mathrm{d}\sigma_{kq}}{\mathrm{d}\omega_t}C_{kq}(\theta_r,\phi_r)^* \tag{9}$$

where $[k]$=2k+1, the angles ω_t=θ_t, ϕ_t and ω_r=θ_r, ϕ_r refer to the coordinates of the unit vectors $\mathbf{k}'$ and $\mathbf{j}'$ along the directions of the product relative velocity angular momentum vectors in the CM frame, respectively. σ is the integral cross section and $\frac{1}{\sigma}\frac{\mathrm{d}\sigma_{kq}}{\mathrm{d}\omega_t}$ are generalized polarization dependent differential cross-sections (PDDCSs), while $C_{kq}(\theta_r,\phi_r)$ are modified spherical harmonics. The differential cross-section (DCS) is given by

$$\begin{aligned} \frac{1}{\sigma}\frac{\mathrm{d}\sigma_{00}}{\mathrm{d}\omega_t} &= P(\omega_t) \\ &= \sum_{k_1}\frac{[k_1]}{4\pi}h_0^{k_1}(k_1,0)P_{k_1}(\cos\theta_t) \end{aligned} \tag{10}$$

The bipolar moments $h_0^{k_1}(k_1,0)$ are evaluated using the expectation values of the Legendre moments of DCS,

$$h_0^{k_1}(k_1,0) = \langle P_{k_1}(\cos\theta_t)\rangle \tag{11}$$

Note that the DCS obtained here only describes the $\mathbf{k}$-$\mathbf{k}'$ correlation or the scattering direction of the product and is not associated with the orientation or alignment of the product rotational angular momentum vector $\mathbf{j}'$.

C. Quasi-classical trajectory calculations

The collision energies are chosen as 1.0, 1.5, 2.0, and 2.5 eV for the title reaction on the PES mentioned above. The vibrational and rotational levels of the reactants molecule are taken as v=0 and j=0, respectively. The accuracy of the numerical integration is verified by checking the conservation of the total energy and total angular momentum for every trajectory. In our calculation, batches of 2×10^4 trajectories are run for the reaction. All trajectories have been calculated starting from an initial separation of 12 Å between the O^+ and the center of mass of the diatomic molecule, because at this distance the interaction energy can be neglected with respect to both the relative energy and the internal energy of the molecule. The initial azimuthal orientation angle and polar angle of the reagent molecule inter-nuclear axis are randomly sampled using Monte Carlo method, and the range of the angles is from 0° to 180° and from 0° to 360°, respectively. The integration step size is chosen as 0.1 fs. For each reaction, the maximal impact parameter $b_{\max}$ is 1.44, 1.71, 1.76, and 1.85 Å, respectively.

DOI:10.1088/1674-0068/23/05/521-526

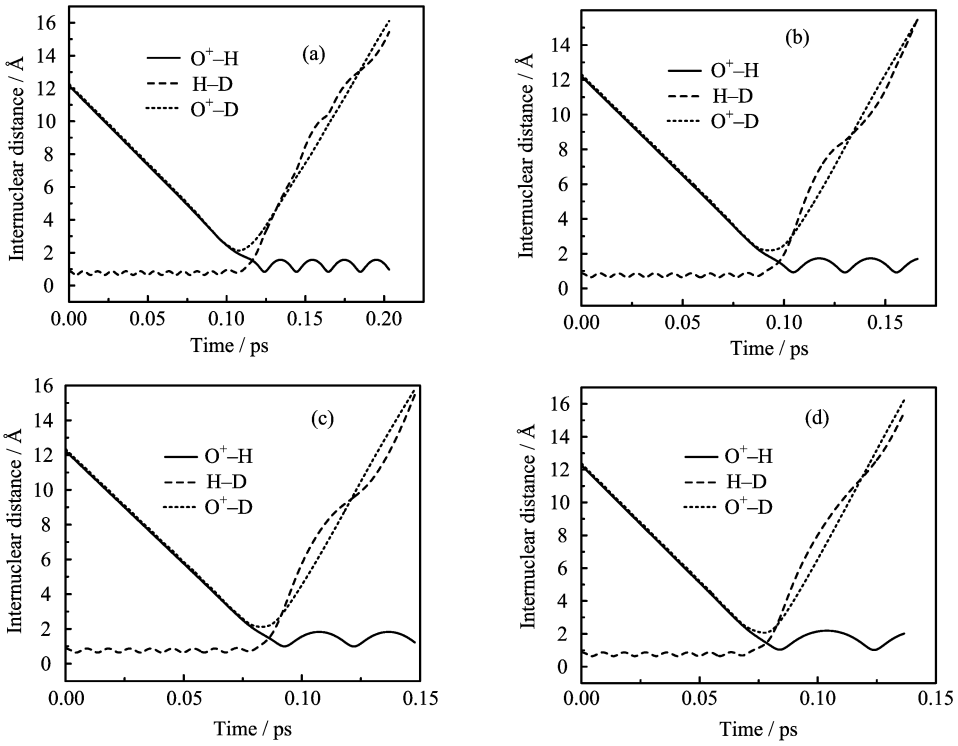

FIG. 2 Internuclear distance of O^+-H, H−D, and O^+-D as a function of propagation time, with the scattering angle of θ_t=141° at E_c=1.0 eV (a), θ_t=124° at E_c=1.50 eV (b), θ_t=102° at E_c=2.0 eV (c), and θ_t=132° at E_c=2.50 eV (d).

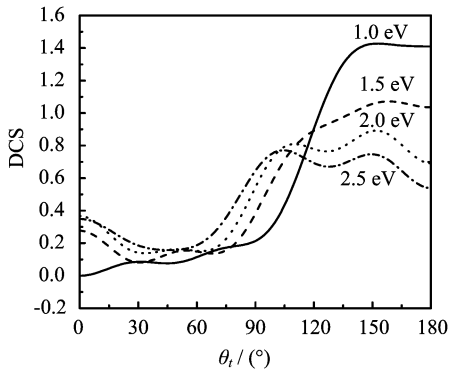

FIG. 3 Differential cross sections for the reaction O^++DH(v=0, j=0)→OD^++H at four collision energies, plotted as a function of scattering angle θ_t.

III. RESULTS AND DISCUSSION

It is of interest to investigate the scattering direction of the product. The DCS derived from the PDDCS offers an excellent opportunity to study chemical reactions at this level of detail. To understand a clear reaction mechanism, the variation of internuclear distances of O^+-H, H−D and O^+-D, are presented as a function of propagation time [24] in Fig.2. The DCS for the reaction O^++DH(v=0, j=0)→OD^++H at selected collision energies (E_c) are shown in Fig.3. At the lower collision energy of 1.0 eV, the DCS shows apparent backward scattering. Figure 3 also shows that the backward scattering decreases rapidly with the increment of energy but the forward scattering increases slightly with the increment of energy.

Figure 2 shows that O^+ collides with the DH molecule and forms an OD^+ that moves away immediately. For each energy, there has a scattering angle which we can see in the result of our calculations. We observed direct reactive trajectories at any collides energy. So, it is no surprise that we observed backward scattering at any collides energy. Thus, we can know that the reaction is dominated by the direct reaction mechanism.

$P(\theta_r)$ distribution of the products which describes the **k**-**j**′ correlation is associated with the collision energy. Figure 4(a) shows that the peak of $P(\theta_r)$ is at θ_r=90° and symmetric with respect to 90°, which suggests that **j**′ is strongly aligned along the direction perpendicular to **k**. The peak of $P(\theta_r)$ becomes higher when the collision energy increases. The result is excellent accordance with the values of product rotational alignment $\langle P_2(\mathbf{j}' \cdot \mathbf{k})\rangle$, which are −0.3505, −0.4297, −0.4505, and −0.4579 at 1.0, 1.5, 2.0, and 2.5 eV, respectively.

$P(\phi_r)$ depicted in Fig.4(b) describe **k**-**k**′-**j** correlations. The peak of $P(\phi_r)$ appears at ϕ_r=270°, which demonstrates that **j**′ is preferentially oriented along the negative direction of the y-axis. According to the previous theoretical study [25] on the molecular reaction

DOI:10.1088/1674-0068/23/05/521-526

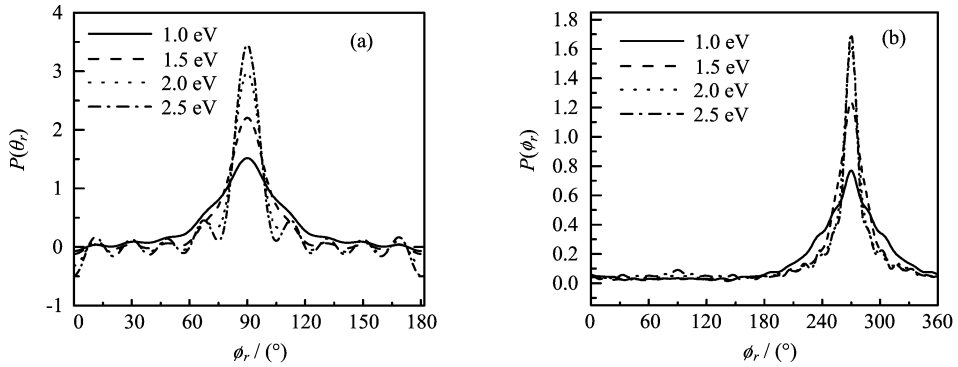

FIG. 4 The angular distribution of $P(\theta_r)$ and $P(\phi_r)$ at four collision energies. (a) The $P(\theta_r)$ describes the **k**-**j**′ correlation. (b) The $P(\phi_r)$ of **j**′ with respect to the **k**-**k**′ plane.

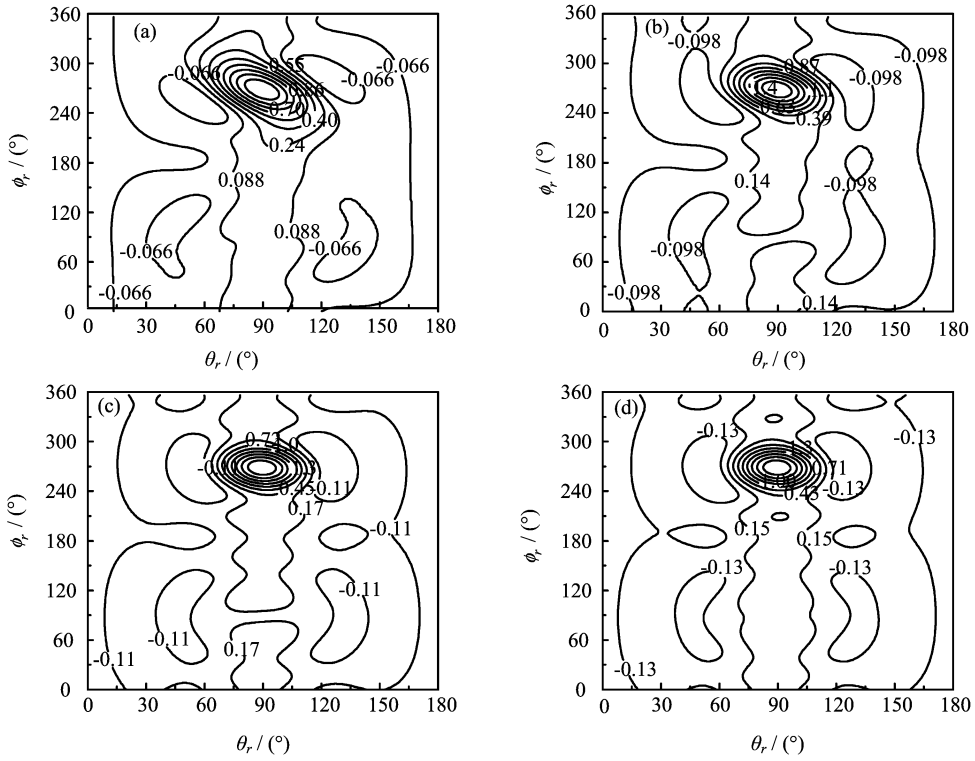

FIG. 5 Polar plots of $P(\theta_r, \phi_r)$ distribution. The collision energies is 1.0 eV (a), 1.5 eV (b), 2.0 eV (c), and 2.5 eV (d), respectively.

for the reaction A+BC→AB+C, we have

$$\mathbf{j}' = \mathbf{L}\sin^2\beta + \mathbf{j}\cos^2\beta + \frac{\mathbf{J}_1 m_{\mathrm{B}}}{m_{\mathrm{AB}}} \tag{12}$$

$$\mathbf{J}_1 = \sqrt{\mu_{\mathrm{BC}} R}\,(\mathbf{r}_{\mathrm{AB}} \times \mathbf{r}_{\mathrm{CB}}) \tag{13}$$

where **L** is the reagent orbital angular momentum, $\mathbf{r}_{\mathrm{AB}}$ and $\mathbf{r}_{\mathrm{CB}}$ are unit vectors where atom A points to atom B and where atom B points to atom C, respectively; μ_{BC} is the reduced mass of the BC molecule and R is the repulsive energy. During chemical-bond forming and breaking for the O^++DH→OD^++H reaction, the term $\mathbf{L}\sin^2\beta$+$\mathbf{J}\cos^2\beta$ in the equation is symmetric, while the term $\mathbf{J}_1 m_{\mathrm{B}}/m_{\mathrm{AB}}$ shows a preferred direction because of the effect of repulsive energy, which leads to the orientation of the product OD^+. The peak at ϕ_r=270° is evidently higher than that at ϕ_r=90° of three collision energies, **j**′ is preferentially oriented along the positive direction of y-axis, and the peak of $P(\phi_r)$ becomes higher when the collision energy increases.

We also plot the angular momentum polarization in the form of polar plot θ_r and ϕ_r at three collision energies in Fig.5. The distributions of $P(\theta_r, \phi_r)$ with peak at (90°, 90°) and (90°, 270°) are in good accordance with the distributions of $P(\theta_r)$ and $P(\phi_r)$ of the products.

DOI:10.1088/1674-0068/23/05/521-526

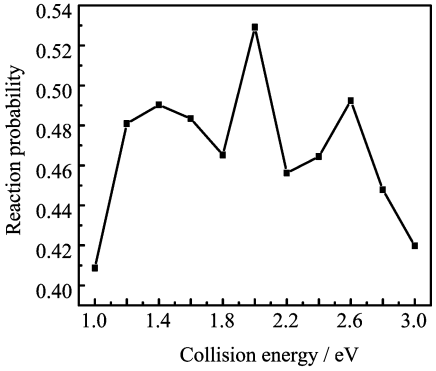

FIG. 6 The reaction probability in this work at different collision energies for the reaction O^++DH(v=0, j=0)→OD^++H.

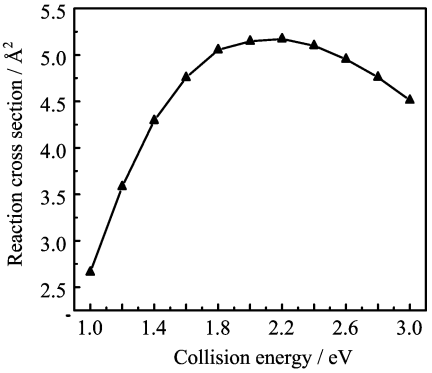

FIG. 7 The reaction cross section for the reaction O^++DH(v=0, j=0)→OD^++H at different collision energies.

Figure 6 shows the results of the reaction probability in our calculation. It is clear that the reaction probability shows different values at different collision energies and has a larger reaction probability at E_c=2.0 eV. From Fig.6 we can see, the reaction probability of this reaction increase considerably with the increase of the collision energy when E_c<2.0 eV, but the reaction probability decrease when E_c>2.6 eV. This phenomenon can be due to the character of our potential energy surface. This reaction is a prototype of moderately exothermic ion-molecule system and potential energy surface has potential well.

The total reaction cross section results are showed in Fig.7. It can be seen that the total reaction cross section increase considerably with the increase of the collision energy when E_c<2.1 eV but the total reaction cross sections decrease slightly when E_c>2.1 eV.

Not only the scalar properties but also the vector properties can be acquired by means of QCT [27]. Because the rotational alignment of the product has solely been measured in most experiments, we only calculated the average rotational alignment factor $\langle P_2(j' \cdot k)\rangle$ (the detailed analysis can be referred in Ref.[27]), and the dependence of the product rotational alignment on collision energies is shown in Fig.8. It can be seen from the figure that the $\langle P_2(\mathbf{j'} \cdot \mathbf{k})\rangle$ values are almost invariant with collision energies, but in detail, the $\langle P_2(\mathbf{j'} \cdot \mathbf{k})\rangle$ value slightly becomes smaller with the collision energy increase, indicating there are weak product rotational alignments and the alignment becomes stronger to some extent when the collision energy increases. In this case we can deduce that the reaction belongs to heavy-light-light mass combination, the product orbital angular momentum is large, and the reactant orbital angular momentum has less influence on the molecular product rotational alignment, which is consistent with the previous calculation [28−33].

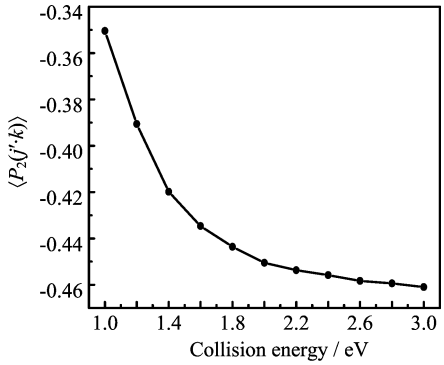

FIG. 8 The product rotational alignment of reaction O^++DH(v=0, j=0)→OD^++H as a function of collision energy.

IV. CONCLUSION

The stereo-dynamics of the reaction O^++DH(v=0, j=0)→OD^++H has been investigated by the QCT method at four collision energies (1.0, 1.5, 2.0, and 2.5 eV). From the calculation we know that the DCS shows apparent backward scattering, and the backward scattering decreases rapidly with the increment of energy. We also observed direct reactive trajectories at any collide energy of this reaction. Thus, we can know that the reaction is dominated by the direct reaction mechanism. $P(\phi_r)$ and $P(\theta_r)$ demonstrate that the rotational polarization of product presents different characters for different collision energies. The rotational angular momentum vectors $\mathbf{j'}$ of the products are not only aligned, but also oriented.

V. ACKNOWLEDGMENTS

This work was supported by the National Natural Science Foundation of China (No.10504017 and No.10874104) and the Key Project of Chinese Ministry of Education. (No.206093). Many thanks to Professor Ke-li Han for providing the QCT code of stereo dynamics.

DOI:10.1088/1674-0068/23/05/521-526

[1] C. Y. Ng, J. Phys. Chem. A **106**, 5953 (2002), and references cited therein.
[2] M. González, M. Gilibert, A. Aguilar, and R. Sayós, J. Chem. Phys. **98**, 2927 (1993), and references cited therein.
[3] F. Illas, P. S. Bagus, J. Rubio, and M. González, J. Chem. Phys. **94**, 3774 (1991), and references therein.
[4] R. Martínez, J. D. Sierra, and M. González, J. Chem. Phys. **123**, 174312 (2005).
[5] M. Rodrigo, J. D. Sierra, and G. Miguel, J. Chem. Phys. **123**, 174312 (2005).
[6] M. Rodrigo, M. Judith, and G. Miguel, J. Chem. Phys. **120**, 4705 (2004).
[7] J. D. Burley, K. M. Ervin, and P. B. Armentrout, Int. J Mass Spectrom. Ion Process. **80**, 152 (1987).
[8] M. Rodrigo, J. M. Lucas, G. Xavier, A. Antonio, and G. Miguel, J. Chem. Phys. **124**, 144301 (2006).
[9] M. Rodrigo, J. D. Sierra, K. G. Stephen, and G. Miguel, J. Chem. Phys. **125**, 164305 (2006).
[10] L. P. Ju, K. L. Han, and Z. H. John Zhang, J. Comput. Chem. **30**, 305 (2009).
[11] W. W. Xu, X. G. Liu, and Q. G. Zhang, Mol. Phys. **106**, 14 (2008).
[12] W. W. Xu, X. G. Liu, S. X. Luan, S. S. Sun, and Q. G. Zhang, Chin. Phys. B **18**, 339 (2009).
[13] W. W. Xu, X. G. Liu, S. X. Luan, and Q. G. Zhang, Chem. Phys. **355**, 21 (2009).
[14] N. C. Blais and D. G. Truhlar, J. Chem. Phys. **67**, 1540 (1977).
[15] A. J. Orr-Ewing and R. N. Zare, Annu. Rev. Phys. Chem. **45**, 315 (1994).
[16] J. Zhao, Y. Xu, and Q. T. Meng, J. Phys. B **42**, 165006 (2009).
[17] Q. T. Meng, J. Zhao, Y. Xu, and D. G. Yue, Chem. Phys. **362**, 65 (2009).
[18] M. Brouard, H. M. Lambert, S. P. Rayner, and J. P. Simons, Mol. Phys. **89**, 403 (1996).
[19] F. J. Aoiz, M. Brouard, V. J. Herrero, V. SaezRabanos, and K. Stark, Chem. Phys. Lett. **264**, 487 (1997).
[20] M. L. Wang, K. L. Han, and G. Z. He, J. Chem. Phys. **109**, 5446 (1998).
[21] M. D. Chen, K. L. Han, and N. Q. Lou, Chem. phys. Lett. **357**, 483 (2002).
[22] M. D. Chen, K. L. Han, and N. Q. Lou, J. Chem. Phys. **118**, 4463 (2003).
[23] J. J. Ma, M. D. Chen, S. L. Cong, and K. L. Han, Chem. Phys. **327**, 529 (2006).
[24] X. H. Li, M. S. Wang, H. Pino, C. L. Yang, and L. Z. Ma, Phys. Chem. Chem. Phys. **11**, 10438 (2009).
[25] K. L. Han, G. Z. He, and N. Q. Lou, Chin. J. Chem. Phys. **2**, 323 (1989).
[26] N. E. Shafer-Ray, A. J. Orr-Ewing, and R. N. Zare, J. Phys. Chem. A **99**, 7591 (1995).
[27] K. L. Han, G. Z. He, and N. Q. Lou, J. Chem. Phys. **105**, 8699 (1996).
[28] M. L. Wang, K. L. Han, and G. Z. He, J. Phys. Chem. A **102**, 10204 (1998).
[29] J. Zhao, Y. Xu, D. G. Yue, and Q. T. Meng, Chem. Phys. Lett. **471**, 160 (2009).
[30] T. S. Chu, Y. Zhang, and K. L. Han, Int. Rev. Phys. Chem. **25**, 201 (2006).
[31] T. S. Chu and K. L. Han, Phys. Chem. Chem. Phys. **10**, 2431 (2008).
[32] R. J. Li, K. L. Han, F. E. Li, R. C. Lu, G. Z. He, and N. Q. Lou, Chem. Phys. Lett. **220**, 281 (1994).
[33] M. González, A. Aguilar, and M. Gilibert, Chem. Phys. **131**, 347 (1989).

DOI:10.1088/1674-0068/23/05/521-526